[Frontiers in Bioscience-Landmark, 8, 312-321, DOI:10.52586/4945] https://www.fbscience.com

Original Research

Evaluation of the efficiency of the imperative ecological remediation regarding tree growth, root development, and edaphic properties after Typhoon Hato (2017) in Zhuhai, China

Chi Zhang[1], Wanhui Qian[1], Lei Song[1], Dongxian Xu[1], Qing Zhao[1,*]

[1]*Guangdong Academy of Forestry, Guangdong Provincial Key Laboratory of Silviculture Protection and Utilization, 510520 Guangzhou, Guangdong, China*

TABLE OF CONTENTS

1. Abstract
2. Introduction
3. Materials and methods
- *3.1 Study area, sampling plots, and tree species selection*
- *3.2 Climatic variables*
- *3.3 Measurement of edaphic conditions*
- *3.4 Measurement of above-ground growth*
- *3.5 Measurement of below-ground progress*
- *3.6 Statistical analysis*

4. Results
- *4.1 Soil physical and chemical properties*
- *4.2 Development of tree height and ground diameter*
- *4.3 Development of fine root biomass*

5. Discussion
- *5.1 Importance of above-ground growth for urban trees*
- *5.2 Root growth patterns from different perspectives*
- *5.3 Impact of ecological remediation on soil physical and chemical properties*
- *5.4 Urban tree species selection for future ecological remediation*

6. Conclusions
7. Author contributions
8. Ethics approval and consent to participate
9. Acknowledgment
10. Funding
11. Conflict of interest
12. References

1. Abstract

Background: urban forest in coastal cities encounters multiple disturbances of frequent typhoon events caused by global change, under which ecological remediation can help to improve urban environment. We measured and analyzed the growth and ecosystem services of four newly-planted tree species in Zhuhai after Typhoon Hato (2017), aiming to evaluate the efficiency of the ecological remediation. **Methods**: National Meteorological Information Center of China supplied climate variables. From June 2018 to December 2019, we measured soil physical and chemical properties, above- and below-ground development regarding stem, tree height, and root growth of all the selected tree species. **Results**: *Sl* (*Sterculia lanceolata* Cav.), *Ir* (*Ilex rotunda* Thunb), *Ss* (*Schima superba* Gardn. et Champ.) could be more wind-resistant from the above-ground morphological perspective. For the below-ground process, Sl was the only tree species with continuous development, while *Ir*, *Ss*, and *Es* (*Elaeocarpus sylvestris* (Lour.)

Submitted: 30 May 2021 Revised: 27 July 2021 Accepted: 3 August 2021 Published: 30 August 2021

Poir.) decreased. Furthermore, *Sl*, *Ir*, and *Ss* maintained their investment in deep roots when *Es* had apparent deep root biomass reduction. The edaphic condition showed notable improvement in chemical properties rather than physical properties, especially for *AN* (available nitrogen), *AK* (available potassium), and *SOM* (soil organic matter). **Conclusions**: The ecological remediation in Zhuhai after Typhoon Hato (2017) was efficient, and in the future, tree species like Sl with advantages in root development and morphological profile were preferentially recommender for plantation in typhoon-affected areas.

2. Introduction

The last decade has witnessed robust evidence that global warming progressively affected human society and natural ecosystems, which also increased the periodicity and intensity of extreme climate events such as heat waves, droughts, tornadoes, and hurricanes [1–3]. Extreme climate events, altering ecosystem structure and function well outside normal variability, attracted increasing attention as drivers of change in ecological and evolutionary communities [4–6]. For example, Stocker *et al*. (2019) [7] applied satellite retrievals of information on the earth's surface to examine the ecological impacts of droughts on global terrestrial photosynthesis and primary production. Elsner *et al*. (2019) [8] quantified the magnitude of the power of tornadoes in consideration of diurnal and seasonal influences embedded within natural variations in the US for the recent 20 years. Besides, it was predicted that El Nino Phenomenon associated with sea-level rise might lead to changes in the frequency and intensity of extreme coastal flood events in Latin America [9]. Researches also developed predictive models to predict how to reduce wind damage in Austrian forests by analyzing remote sensing images [10].

Researches have consistently been conducted on the impact of various extreme climate events on human society or ecosystems, however, the efficiency of people's subsequent ecological remediation was scarcely investigated [11]. Furthermore, it might not be comprehensively and thoroughly answered whether the ecological remediation could enhance our capacity of coping with similar extreme climate events in the future from the perspectives of tree physiological development in China [12]. For example, Zhuhai, a coastal city located in southeastern China, frequently confronts typhoon events every several years. Although the local ecological department invariably implemented ecological remediation after every typhoon left, lack of evaluation of the quality of their remediation coupled with neglect of subsequent adaptation could probably expose the city to typhoon damage again, partly resulting in exponentially increasing economic losses as well as rising numbers of injuries. Therefore, pertinent evaluation and specific recommendations could be positive efforts for those typhoon-suffering areas to enhance their abilities of resisting multiple natural disturbances.

Urban forests and trees, providing multiple ecosystem services such as improving urban air quality, reducing noise, attenuating storm-water flooding, and conserving energy, could be a key component in the adaptation of cities to climate change [13–15]. In addition, the plantation of urban trees was generally considered to effectively help cities acclimate to extreme climate events, especially for ecological remediation after typhoon events [16]. This was because urban trees played a crucial role in promoting both above- and below-ground processes such as recovering in soil fertility, water conservation, construct and improve environmental conditions, which was most likely damaged or affected by fierce winds and intense rainfalls [17–19]. Hence, detailed information regarding the development of those urban trees planted for ecological remediation could contribute potently to a profound understanding of the efficiency of remediation and future prediction.

Zhuhai city, suffering severely from Typhoon Hato (2017), implemented imperative ecological remediation via tree species selection and urban tree plantation in June 2018. Nevertheless, the remediation was principally from political perspectives and carried out by the local administrative department, which might lack scientific assessment, hampering a profound understanding of the quality of the remediation progress. Therefore, we selected the remediation district encountering Typhoon Hato as our objected area and established both above- and below-ground measurements for the newly-planted tree species. Additionally, with environmental data, we expected to answer questions as following: (1) whether did the newly-planted trees adapt to the local environment regarding their growth patterns? (2) How did the selected tree species develop their fine root biomass in vertical and horizontal levels? (3) Under the ecological remediation, was the edaphic condition improved in terms of physical and chemical properties? (4) what kind of tree species could be recommended in typhoon-affected areas?

3. Materials and methods

3.1 Study area, sampling plots, and tree species selection

Located in the southeastern coastal areas of China, Zhuhai is frequently confronted with extreme climate events as typhoons' disturbance (Fig. 1). On 20th August 2017, Typhoon Hato generated upon the northwestern Pacific Ocean and constantly intensified within 72 h. At 12:50 on 23rd August, it landed on Zhuhai at wind scale 14 and moved forward in the northwest direction. During its route in Zhuhai lasting over 4 h, more than 25% of urban trees in quantitative terms in Zhuhai were damaged by the strong wind. After Typhoon Hato left, imperative ecological remediation was planned and launched according to the prac-

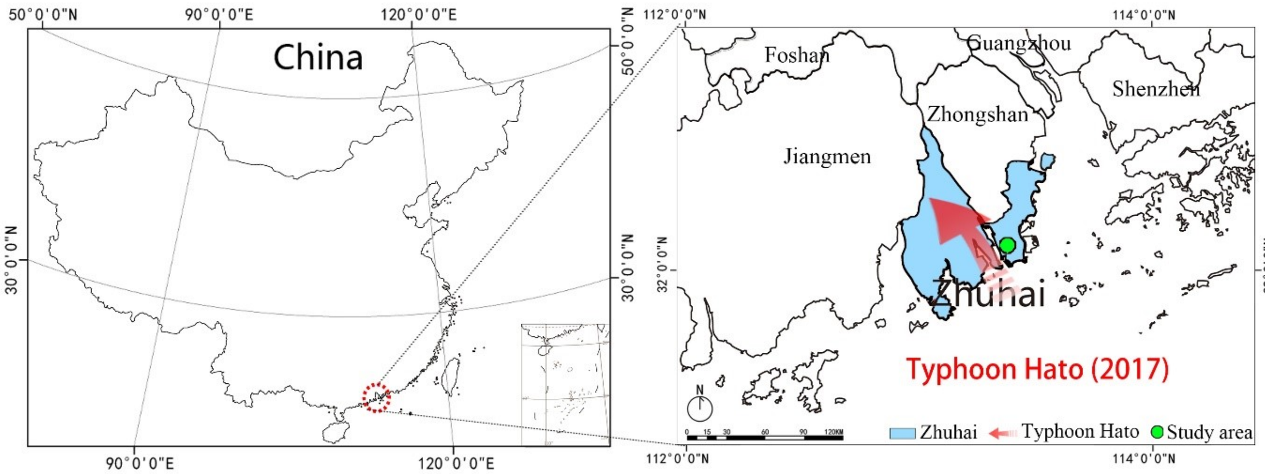

Fig. 1. Schematic of Zhuhai in China (blue area with red framework), landing location and route of Typhoon Hato (broad red arrow), and location of our study area in Zhuhai (green area).

tical condition in each area. In Xiangzhou district, which suffered enormously from the typhoon disturbance, the local forestry administration department took several steps to recover and re-build urban greening, including sweeping typhoon-affected areas, restoring land and soil, and making ecological restoration plans. In June 2018, 18 indigenous tree species were selected and over 50,000 saplings were planted. To analyze their growing conditions that helped to evaluate the quality of the imperative ecological remediation, we selected four most-planted tree species as our objects within the whole planting area, i.e., *Sterculia lanceolata* Cav. (*Sl*), *Ilex rotunda* Thunb (*Ir*), *Schima superba* Gardn. et Champ. (*Ss*), and *Elaeocarpus sylvestris* (Lour.) Poir. (*Es*). The four tree species are all native tree species with flexible soil adaption. In order to select the most representative trees of the four tree species, five sampling plots with the size of 30 $\times$ 30 m were randomly established. In each sampling plot, all the trees were surveyed and their data of tree height and ground diameter was recorded, based on which four sampling trees of each tree species were determined. The measurements on all the 16 trees were conducted in June 2018, December 2018, June 2019, and December 2019, i.e., trees' ages at 0 months (0M), six months (6M), 12 months (12M), and 18 months (18M).

3.2 Climatic variables

National Meteorological Information Center of China (http://data.cma.cn) supplied climate data, based on which monthly climatic variables including wind velocity (km h^{-1}), precipitation (mm), and temperature (°C) were collected and calculated from January 2017 to December 2019 in Zhuhai. As a coastal city under a subtropical and tropical maritime climate, Zhuhai had a relatively high average temperature at 22.5 °C and plenty of precipitation over 2000 mm annually from 1995 to 2015. From 2017 to 2019, the average wind velocity slightly fluctuated around 10 km h^{-1} while the highest wind velocity would reach over 100 km h^{-1}, primarily when extreme climatic events occurred. In August 2017, Typhoon Hato landed in the southeast coastal areas of China and intruded the front of Zhuhai city, resulting in the monthly highest wind velocity and precipitation reaching 217 km h^{-1} and 277 mm.

3.3 Measurement of edaphic conditions

The primary soil type in Zhuhai is red acidic soil. The soil sampling campaign was launched in the study area in June 2018 and December 2019 to indicate the development of soil physical and chemical properties. For each time, five metallic-cylindrical sampling cores were used to dig out two kilos of soil in the depth of 30 cm, which were randomly located in the study area same as the sampling plots. Then all the soil samples were well kept in sampling bags and transported to our laboratory for further analysis. The soil's physical properties were measured according to Li and Shao's reports [20]. Soil bulk densities (*BD*, g cm^{-3}) were determined by the mass of soil per unit volume (sum of solids and pore space) and the soil cores were oven-dried at 105 °C to obtain soil moisture content (*SMC*, %). Then, the soil cores were put on a sand salver and allowed to drain for 2 h in order to calculate soil capillary water content (*Scwc*). Hence, soil capillary porosity (*Scp*, %) was calculated according to the equation as:

$$Scp = 0.1 \times Scwc \times ds \tag{1}$$

where ds is the soil density (mg m^{-3}). And soil non-capillary porosity (*Sncp*, %) and soil total porosity (*Stp*, %) were calculated as:

$$\begin{aligned} Sncp &= 0.1 \times (Smc - Scwc) \times ds \\ Stp &= Scp + Sncp \end{aligned} \quad (2)$$

For soil chemical properties, soil PH was determined in 1 : 2.5 soil-water slurry using a combination glass electrode. Soil organic matter (*SOM*, g kg^{-1}) was determined by the oil bath-$K_2Cr_2O_7$ titration method. Total nitrogen (*TN*, g kg^{-1}) was determined by the semi-micro Kjeldahl method. Available nitrogen (*AN*, mg kg^{-1}) was determined by a micro-diffusion technique after alkaline hydrolysis. Total phosphorus (*TP*, g kg^{-1}) was determined colorimetrically after wet digestion with H_2SO_4 + $HClO_4$. Available phosphorus (*AP*, mg kg^{-1}) was exacted with 0.5 mol l^{-1} $NaHCO_3$ solution (PH 8.5). Total potassium (*TK*, g kg^{-1}) was determined by the Cornfield method. Available potassium (*AK*, mg kg^{-1}) was determined by the CH_3COONH_4 extraction method [21].

3.4 Measurement of above-ground growth

In June 2018, the saplings of all the tree species were simultaneously planted in the study area, which had unified short and small sizes (height around 25 cm and DBH around 0.5 cm). Therefore, the four tree species were considered to have the completely same and tiny initial conditions. To investigate their above-ground growth, their ground diameters were measured with the help of a vernier caliper (Altraco Inc., Sausalito, California, USA) and their height was measured using a standard tape. The measurement was conducted in December 2018, June 2019, and December 2019 to explore the above-ground development patterns from 0M to 18M.

3.5 Measurement of below-ground progress

To clarify the below-ground progress, fine root coring campaigns were launched for all the selected trees at the same time as the above-ground measurement. A pre-test coring campaign showed that the range of the root system was similar to a cylinder, with a diameter of 70 cm and a height of 35 cm. Therefore, for the 16 trees, eight soil cores were collected for every individual tree: four at a distance of 15 cm from the trunk and the other four at 30 cm. The soil was sampled down to a depth of 30 cm using a soil auger with a length of 30 cm and a radius of 3 cm. Each sample was divided into three horizons: soil depths of 0–10 cm (upper layer), 10–20 cm (middle layer), and 20–30 cm (deep layer). Fine roots ($<$2 mm) were filtered using sieves (2-mm mesh size) and separated by forceps in the laboratory. Then, the samples were washed and dried in an oven at 65 °C for 72 h. Finally, all the samples were weighed using a balance with an accuracy of four decimal places to obtain the dry weight. The fine root biomass at different depths was calculated using the dry weight divided by the cross-sectional area of the auger.

3.6 Statistical analysis

The software SPSS 22.0 (IBM, State of New York, USA) was used for statistical analysis. To investigate the difference between means, two-sampled *t*-test and analysis of variance (ANOVA) with Tukey's HSD (honestly significant difference) test were used. In all the cases, the means were reported as significant when $P < 0.05$. Where necessary, data were log or power transformed in order to correct for data displaying heteroscedasticity.

4. Results

4.1 Soil physical and chemical properties

Five physical and eight chemical variables were measured to analyze the soil revolution under the ecological remediation (Table 1). For physical properties, no significant difference was detected between June 2017 and December 2019, among which *SMC* and *BD* exhibited slight decreases (from 22.64% ± 1.90% to 19.90% ± 2.82%; from 1.28 ± 0.06 to 1.23 ± 0.06 g cm^{-3}). In terms of soil porosity, all the three variables, *Stp*, *Scp*, and *Sncp* increased distinctly. For chemical properties, except for *TN* (from 1.02 ± 0.25 to 1.01 ± 0.23 g kg^{-1}), the other variables displayed apparent development, especially for *AN*, *AK*, *SOM* showing drastic upsurge (from 47.78 ± 16.91 to 152.60 ± 21.05 mg kg^{-1}; from 18.18 ± 9.56 to 85.80 ± 27.62 mg kg^{-1}; from 10.36 ± 3.32 to 18.44 ± 3.67 g kg^{-1}). Besides, soil acidity reduced with PH values decreasing from 4.20 ± 0.04 to 5.04 ± 0.74.

4.2 Development of tree height and ground diameter

Under the same initial condition (all the four tree species were short and small saplings.), the four tree species displayed different growing patterns regarding tree height and ground diameter (Fig. 2). *Es* had the most rapid growth of tree height for the whole period and reached 2.98 ± 0.61 m at 18M. In addition, it also had the second-highest value of ground diameter (5.15 ± 0.78 cm) among the four tree species. Both *Sl* and *Ir* increased their tree height sharply within the first six months (0.88 ± 0.10 m; 1.3 ± 0.12 m), which turned gradual growth from 6M to 18M. However, we observed that *Sl* had the largest ground diameter (5.80 ± 0.39 cm), which mainly originated from its dramatic development from 12M to 18M. In comparison to others, *Ss* exhibited disadvantages in growing rates regarding both height and diameter, which reached 2.07 ± 0.20 m and 4.80 ± 0.56 cm at 18M.

4.3 Development of fine root biomass

4.3.1 Total fine root biomass

Four tree species displayed different fine root growth patterns for the whole period (Fig. 3). During the first six months, they showed no significant differences (19.64 ± 17.92 g m^{-2}; 21.81 ± 18.49 g m^{-2}; 11.20 ± 13.17

Table 1. Measured soil physical and chemical properties.

Soil properties		n	Date	
			June 2018	December 2019
Physical properties	*SMC* (%)	5	22.64 ± 1.90	19.90 ± 2.82
	Stp (%)	5	39.80 ± 2.66	45.72 ± 9.14
	Scp (%)	5	35.66 ± 2.86	39.31 ± 4.77
	Sncp (%)	5	4.14 ± 1.65	6.41 ± 1.34
	BD (g cm^{-3})	5	1.28 ± 0.06	1.23 ± 0.06
Chemical properties	*TN* (g kg^{-1})	5	1.02 ± 0.25	1.01 ± 0.23
	TP (g kg^{-1})	5	0.26 ± 0.10	0.31 ± 0.14
	TK (g kg^{-1})	5	15.40 ± 4.78	21.52 ± 6.89
	AN (mg kg^{-1})	5	47.78 ± 16.91 *	152.60 ± 21.05 *
	AP (mg kg^{-1})	5	1.08 ± 0.19	1.09 ± 0.17
	AK (mg kg^{-1})	5	18.18 ± 9.56 *	85.80 ± 27.62 *
	PH	5	4.20 ± 0.04	5.04 ± 0.74
	SOM (g kg^{-1})	5	10.36 ± 3.32 *	18.44 ± 3.67 *

Soil moisture content (SMC, %), soil total porosity (Stp, %), soil capillary porosity (Scp, %), soil non-capillary porosity (Sncp, %), bulk density (BD, g cm^{-3}), and chemical properties including PH values, soil organic matter (SOM, g kg^{-1}), total nitrogen (TN, g kg^{-1}), total phosphorus (TP, g kg^{-1}), total potassium (TK, g kg^{-1}), available nitrogen (AN, mg kg^{-1}), available phosphorus (AP, mg kg^{-1}), available potassium (AK, mg kg^{-1}). The symbol '*' indicates significant differences ($P < 0.05$) between the measurement in June 2018 and December 2019.

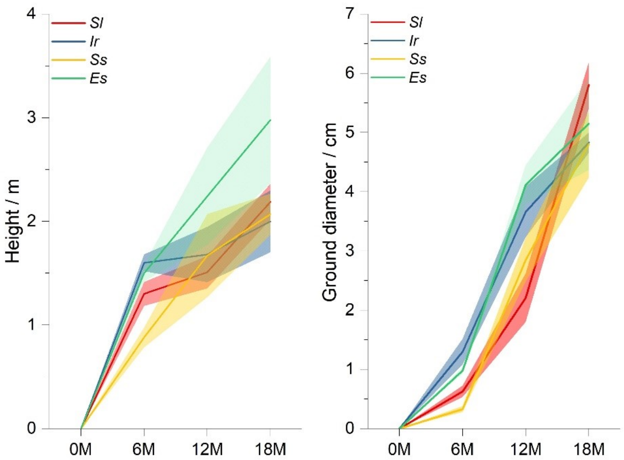

Fig. 2. Development of tree height (m) and ground diameter (cm) of *Sl* (red line), *Ir* (blue line), *Ss* (orange line), and *Es* (green line) from June 2018 (0 months, 0M) to December 2019 (18 months, 18M), around which the light red, blue, orange, and green shading areas are the 95% confidence intervals, respectively.

g m^{-2}; 21.38 ± 25.68 g m^{-2}). From 6M to 12M, all of them obtained dramatic development (229.06 ± 136.12 g m^{-2}; 290.64 ± 133.99 g m^{-2}; 244.43 ± 143.74 g m^{-2}; 415.63 ± 184.29 g m^{-2}), among which *Es* had the most significant increase by 1844.01%. Nevertheless, except that *Sl* maintained growth by 17.59%, the other three tree species had pronounced reductions of their biomass (240.06 ± 119.40 g m^{-2}; 215.70 ± 137.11 g m^{-2}; 248.52 ± 136.73 g m^{-2}), which showed complete opposite fine root growth patterns.

4.3.2 Fine root growth in the vertical level

To clarify the vertical fine root growth for the whole period, we divided them into three layers, i.e., 0–10 cm (shallow layer), 10–20 cm (medium layer), and 20–30 cm (deep layer) (Fig. 4). From December 2018 to June 2019 (6M to 12M), fine root from the three different layers of all the four tree species obtained rapid and dramatic development ($P < 0.05$), especially for the 20–30-cm layer of *Ir* (from 0.20 ± 0.40 g m^{-2} to 64.54 ± 54.65 g m^{-2}), the 10–20-cm layer of *Es* (from 4.34 ± 12.73 g m^{-2} to 158.97 ± 92.27 g m^{-2}), and the 20–30-cm layer of *Es* (from 2.57 ± 12.89 g m^{-2} to 92.27 ± 84.81 g m^{-2}). From June 2019 to December 2019 (12M to 18M), merely *Sl* maintained slight growth in the 0–10-cm layer while other tree species had fine root biomass loss at various levels, e.g., the 0–10-cm layer of *Ir* (from 122.93 ± 75.28 g m^{-2} to 91.39 ± 62.74 g m^{-2}), 10–20-cm layer of *Ss* (from 92.17 ± 65.26 g m^{-2} to 77.99 ± 75.49 g m^{-2}). The greatest reduction of fine root biomass was from the shallow and medium layers of *Es* (from 164.39 ± 115.67 g m^{-2} to 86.66 ± 87.91 g m^{-2}; from 158.97 ± 85.37 g m^{-2} to 92.53 ± 67.79 g m^{-2}), which showed significant difference ($P < 0.05$).

4.3.3 Fine root growth in horizontal level

Fine root biomass from 15 cm (nearby root) and 30 cm (outmost root) to trunk provided us a perspective on the root's horizontal development (Fig. 5). From 6M to 12M, *Sl*, *Ir*, and *Ss* had more root growth at 15 cm than 30 cm, e.g., the nearby root of *Ir* (229.06 ± 136.12 g m^{-2}) and outmost root of *Ir* (229.06 ± 136.12 g m^{-2}). On the contrary, *Es* had a relatively balanced investment in the horizontal

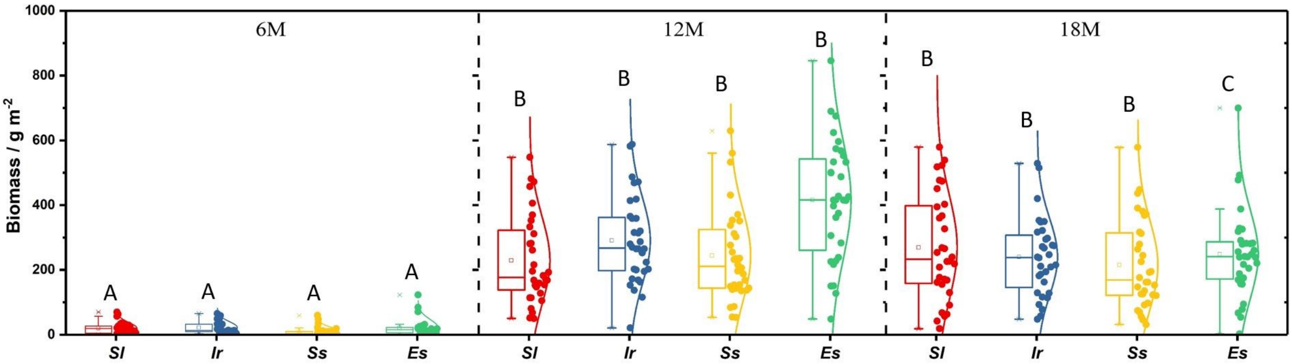

Fig. 3. Development of total fine root biomass (g m^{-2}) of *Sl* (red), *Ir* (blue), *Ss* (orange), and *Es* (green) from December 2018 (6M) to December 2019 (18M). For each tree species, the left box-plot displays the mean value, the median value, and the quartiles, and the right density plot shows the distribution of all the values. For each tree species, the different capital letters indicate significant differences ($P < 0.05$) between biomass at different months.

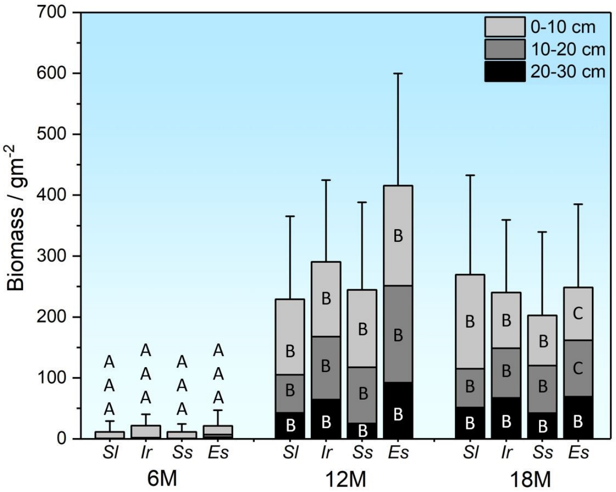

Fig. 4. Vertical development of fine root biomass (g m^{-2}) of *Sl*, *Ir*, *Ss*, and *Es* from December 2018 (6M) to December 2019 (18M). Light grey, medium grey, and black bars represent the fine roots in the soil layer of 0–10 cm, 10–20 cm, and 20–30 cm, respectively. The different capital letters indicate significant differences ($P < 0.05$) between fine root biomass in different months for each layer of each tree species.

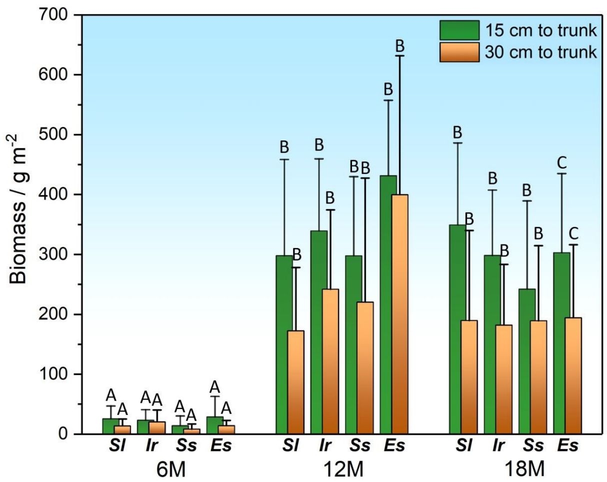

Fig. 5. Horizontal development of fine root biomass (g m^{-2}) of *Sl*, *Ir*, *Ss*, and *Es* from December 2018 (6M) to December 2019 (18M). Green and brown bars represent the fine roots located at 15 cm and 30 cm to tree trunks, respectively. For each tree species, the different capital letters indicate significant differences ($P < 0.05$) between biomass in different months.

level (nearby root: 431.54 ± 125.86 g m^{-2}; outmost root: 399.72 ± 231.97 g m^{-2}). From 12M to 18M, except for *Sl* (nearby root: from 285.64 ± 142.51 g m^{-2}to 349.16 ± 137.09 g m^{-2}; outmost root: from 172.49 ± 105.63 g m^{-2} to 189.56 ± 150.51 g m^{-2}), the other three tree species had different levels of biomass reduction. The fine root biomass at 15 cm and 30 cm of *Ir* and *Ss* were synchronously and approximately reduced, however, *Es* had more biomass loss from outmost root (from 431.54 ± 125.86 g m^{-2} to 302.93 ± 132.11 g m^{-2}) than nearby root (from 399.72 ± 231.97 g m^{-2} to 194.12 ± 121.94 g m^{-2}), showing significant differences ($P < 0.05$).

5. Discussion

5.1 Importance of above-ground growth for urban trees

Numerous studies verified that above-ground growth patterns could reflect trees' health condition, geographic adaptation, and supplying ecosystem services [22–24]. In our research, the growth of tree height and ground diameter for the four tree species were measured from 0M to 18M. Although all of them exhibited a general increase, different periodic patterns implied trees' particular above-ground strategies. *Es* was distinguished for its height growth among the four tree species, implying a robust above-ground construction coupled with its second-highest value of ground diameter, which was in line with the previous findings [25, 26]. On the contrary, the other three tree species exhibited an inclination to develop ground diameter than height. Their height growth primarily occurred from 0M to 12M and slowed down from 12M to 18M, while the ground diameters increased sharply from 6M to 18M. Such growth pattern indicated a stable above-ground morphological profile, which could effectively provide wind-damage resistance that lower but thicker trees might now easily break down in typhoon or hurricane events [27]. This might also be verified by using convolutional neural networks to estimate the relationships between tree failures due to high winds and tree sizes [28]. As showed in Fig. 2, preferential growth of *Sl* was distinctly given to ground diameter to effectually make the above-ground tree profile stable, which could be expected to have higher survival rates under typhoon disturbances in the future.

5.2 Root growth patterns from different perspectives

As the primary pathway for water and nutrient uptake, fine roots were a prominent sink for carbon acquired in terrestrial net primary productivity, tightly related to multiple ecosystem services [29–31]. In our research, we not only measured the total fine root biomass but also the root biomass development in both horizontal and vertical levels, aiming to investigate their absorption capacity of water and nutrient and morphological patterns.

For total fine root biomass, *Sl* was the only tree species growing within the whole 18 months, showing a persistent below-ground investment. Distinct growth occurred within the first year since plantation, however, the other three tree species showed a biomass reduction from 12M to 18M. Combined with their height and ground diameter growth, it could be explained by their specific allocation strategy between the above- and below-ground processes. Generally, urban trees dynamically adjusted the above- and below-ground investment on the basis of their characteristics and environmental conditions [32, 33], such as enhancing above-ground growth for more photosynthesis or increasing root growth for water and nutrients uptake [34–36]. Nevertheless, *Es*'s remarkable decrease of fine root biomass showed a weakened below-ground growth, which could be deeply worried about its adaption in the future. This was because typhoons usually broke down or shaded tree trunks, leading to more severely damaged root systems. In addition, site conditions in typhoon-affected areas were generally fragile and negative that soil quality were highly reduced and ecosystem flow were disturbed, making the fine roots require a lengthy period for recovery [36, 37].

For fine root biomass in the vertical level, the four tree species had significant growth from 0M to 12M (Fig. 4). Similar decreasing patterns from 12M to 18M were found as the total fine root biomass, however, several positive phenomena existed in their deep root layer, i.e., 20–30 cm. As shown in Fig. 6, Zhuhai usually had more than six months with precipitation lower than 100 mm every year and its highest temperature from May to October reached over 30 °C, revealing a hot and dry climate condition which could result in the trees being exposed to water stress. Previous research reported that deep roots could be of pivotal importance for various plants to alleviate water stress, absorb more nutrients, and enhance tree stability [29, 38], particularly play a central role in the tropical and subtropical environment [39]. Therefore, the increase of deep roots of *Sl*, *Ir*, and *Ss* could be practical approaches than *Es* in coping with dry environmental conditions, which was consistent with the results of [40].

Roots' growth in horizontal level was closely relevant to its stabilization, which was essential for those trees confronting typhoon disturbance [41, 42]. In general, trees with higher proportion of outmost roots would be more stable than those with stem-centered roots from the morphological perspective [43]. Nevertheless, the outmost roots might be abandoned priorly when the whole roots system faced shrinkage, such as *Es* from 12M to 18M. From this point of view, it could support that *Ss* tended to be steadier in a typhoon event among the four tree species as it had relatively balanced investment on both nearby and outmost fine roots within the whole study period, even when fine roots died.

5.3 Impact of ecological remediation on soil physical and chemical properties

Vegetation was generally regarded to have substantial potential in soil restoration for cities suffering from extreme climate events [44–46]. Comparing the edaphic conditions in June 2017 and December 2018, the impact of the ecological remediation on local soils could be evaluated in terms of physical and chemical properties. For physical properties, all the variables showed no significant differences that *SMC* and *BD* slightly decreased and *Stp*, *Scp*, and *Sncp* increased to a small extent, implying the ecological remediation rarely influenced the edaphic physical structure. Regarding chemical properties, all the variables displayed escalation, notably for *AN*, *AK*, and *SOM* ($P < 0.05$). As fine root growth would actively participate in edaphic chemical evolution and promote the release of microelement [47], it could give the explanation of the soil improvement. No significant difference was found for *TP* and *AP*, which was probably due to the inactive nature of phosphorus, especially in acidic conditions [48]. Overall, after the typhoon event, the ecological remediation had positive effects on soil chemical properties rather than physical ones within the first 18 months.

5.4 Urban tree species selection for future ecological remediation

Accounting for the complicated interaction between the restricted urban space (compacted soil, complex microclimate, multiple human activities) and the fragmentized environment under the extreme climate events' dis-

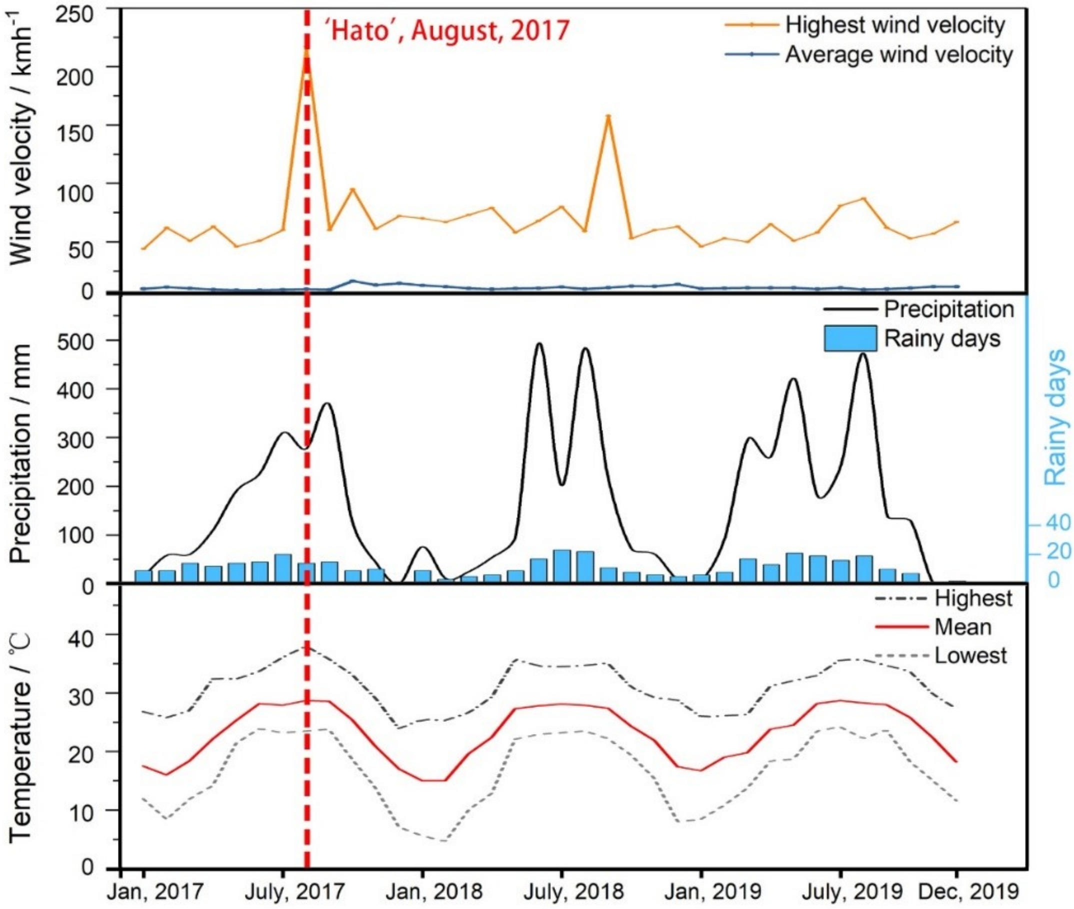

Fig. 6. Monthly climate variables including highest wind velocities (km h^{-1}), average wind velocities (m s^{-1}), precipitation (mm), number of rainy days, highest temperature (°C), mean temperature (°C), and lowest temperature (°C) for Zhuhai from January 2017 to December 2019. The vertical-red-dotted line indicates when Typhoon Hato arrived at Zhuhai city.

turbance [49–52], the efficiency of ecological remediation was essential and urgent from different perspectives. Urban trees could mitigate environmental degradation and provide multiple ecosystem services, specifically for cities encountering extreme climate events, which played a central role in ecological remediation [13]. Their above- and below-ground processes were closely related to their survival rates, morphological growth, geographic adaption, water absorption, and edaphic improvement, which primarily reflected the quality of the ecological remediation [53]. In this study, the selected four tree species showed no deaths but growth, together with which edaphic chemical variables exhibited several improvements. It could be inferred that the ecological remediation in Zhuhai after Typhoon Hato (2017) was effective. However, it still could be improved according to specific growth conditions of different tree species. For example, *Ir*, *Ss*, and *Es* reduced fine root biomass from 12M to 18M, which could be paid more attention to, such as specific fertilization to promote their root growth in this period. We observed that *Sl* had a relatively thicker tree trunk accompanying steady development of total and deep fine root biomass. This could be inferred that *Sl* had morphological and physiological resistance to typhoon events, which could be recommended for future plantation in Zhuhai or be preferentially considered for future ecological remediation to obtain promoted ecosystem services.

6. Conclusions

After Typhoon Hato (2017) intruded on Zhuhai city and severely damaged its urban environment, the local administrative department planned and launched imperative ecological remediation via planting plenty of trees. Aiming to evaluate the efficiency and make relevant suggestions, we measured the above- and below-ground growth of four tree species (*Sl*, *Ir*, *Ss*, *Es*) together with the edaphic evolution in terms of physical and chemical properties.

For the above-ground process, *Es* had advantageous growth with the highest value of tree height and second-highest value of ground diameter. The other three tree species exhibited inclinations to develop ground diameter than height, which were probably more wind-resistant from the morphological perspective. For the below-ground process, *Sl* was the only tree species that obtained continuous development, while *Ir*, *Ss*, and *Es* decreased from 12M to 18M. Besides, *Sl*, *Ir*, and *Ss* maintained their investment in deep roots when *Es* had significant deep root biomass reduction. In the horizontal level, *Ss* had the highest proportion of outmost roots among the four tree species.

After 18 months since the ecological remediation started, the eight physical variables showed minor changes, implying the ecological remediation rarely influenced the edaphic physical structure. However, all the variables displayed escalation, notably for *AN*, *AK*, and *SOM*, which could be attributed primarily to fine roots' participation in edaphic chemical evolution and promote the release of microelement.

In conclusion, the ecological remediation effectively improved the environmental quality via the plantation of various trees in Zhuhai. In the future, the selection of planted trees could be more reliable through a comprehensive analysis of the above- and below-ground processes. Those tree species like *Sl* with advantages in root development and morphological profile are preferentially recommender for plantation in typhoon-affected areas.

7. Author contributions

CZ: conception and design; acquisition of data; analysis and interpretation of data; drafting the manuscript; making figures and tables. WQ, LS and DX: acquisition of data; making figures and tables; acquisition of funding. QZ: Acquisition of funding; Project administration.

8. Ethics approval and consent to participate

Not applicable.

9. Acknowledgment

We greatly appreciate Dajun Guo, Xiu Chen, Qifei Pan, Weiyi Huang, Yuqi Li, Qing Yang, Qiuxia Pan, and Rongchang Nie for their assistance in the collection and calculation of fine root biomass, tree measurement, and soil coring campaign.

10. Funding

This research was funded by the Forestry Science and Technology Innovational Specific Project of Guangdong Province, grant number (2018KJCX029) and (2020KJCX006), and by the Forestry Science and Technology Program of Guangdong Province, grant number (2019-21).

11. Conflict of interest

The authors declare no conflict of interest.

12. References

[1] Ummenhofer CC, Meehl GA. Extreme weather and climate events with ecological relevance: a review. Philosophical Transactions of the Royal Society B: Biological Sciences. 2017; 372: 20160135.
[2] Easterling DR, Evans JL, Groisman PY, Karl TR, Kunkel KE, Ambenje P. Observed variability and trends in extreme climate events: a brief review. Bulletin of the American Meteorological Society. 2000; 81: 417–426.
[3] Diffenbaugh NS, Singh D, Mankin JS, Horton DE, Swain DL, Touma D, *et al.* Quantifying the influence of global warming on unprecedented extreme climate events. Proceedings of the National Academy of Sciences. 2017; 114: 4881–4886.
[4] O'Neill BC, Oppenheimer M, Warren R, Hallegatte S, Kopp RE, Pörtner HO, *et al.* IPCC reasons for concern regarding climate change risks. Nature Climate Change. 2017; 7: 28–37.
[5] Van de Pol M, Jenouvrier S, Cornelissen JH, Visser ME. Behavioural, ecological and evolutionary responses to extreme climatic events: challenges and directions. Philosophical Transactions of the Royal Society of London. Series B, Biological Sciences. 2017; 372: 20160134.
[6] Babcock RC, Bustamante RH, Fulton EA, Fulton DJ, Haywood MD, Hobday AJ, *et al.* Severe continental-scale impacts of climate change are happening now: Extreme climate events impact marine habitat forming communities along 45% of Australia's coast. Frontiers in Marine Science. 2019; 6: 411.
[7] Stocker BD, Zscheischler J, Keenan TF, Prentice IC, Seneviratne SI, Peñuelas J. Drought impacts on terrestrial primary production underestimated by satellite monitoring. Nature Geoscience. 2019; 12: 264–270.
[8] Elsner JB, Fricker T, Schroder Z. Increasingly powerful tornadoes in the United States. Geophysical Research Letters. 2019; 46: 392–398.
[9] Reguero BG, Losada IJ, Diaz-Simal P, Mendez FJ, Beck MW. Effects of climate change on exposure to coastal flooding in Latin America and the Caribbean. PLoS ONE. 2015; 10: e0133409.
[10] Pasztor F, Matulla C, Zuvela-Aloise M, Rammer W, Lexer MJ. Developing predictive models of wind damage in Austrian forests. Annals of Forest Science. 2015; 72: 289–301.
[11] Harris JA, Hobbs RJ, Higgs E, Aronson J. Ecological restoration and global climate change. Hoboken: Wiley Online Library. 2006.
[12] Burger J, Carletta MA, Lowrie K, Miller KT, Greenberg M. Assessing ecological resources for remediation and future land uses on contaminated lands. Environmental Management. 2004; 34: 1–10.
[13] Roy S, Byrne J, Pickering C. A systematic quantitative review of urban tree benefits, costs, and assessment methods across cities in different climatic zones. Urban Forestry & Urban Greening. 2012; 11: 351–363.
[14] Miller RW, Hauer RJ, Werner LP. Urban forestry: planning and managing urban greenspaces. Long Grove: Waveland press. 2015.
[15] Endreny TA. Strategically growing the urban forest will improve our world. Nature Communications. 2018; 9: 1–3.
[16] Yamaki K. Role of social networks in urban forest management collaboration: A case study in northern Japan. Urban Forestry & Urban Greening. 2016; 18: 212–220.
[17] Hamberg L, Malmivaara-Lämsä M, Lehvävirta S, Kotze DJ. The effects of soil fertility on the abundance of rowan (Sorbus aucuparia L.) in urban forests. Plant Ecology. 2009; 204: 21–32.

[18] Dwyer JF, McPherson EG, Schroeder HW, Rowntree RA. Assessing the benefits and costs of the urban forest. Journal of Arboriculture. 1992; 18: 227–234.
[19] Jim CY, Chen WY. Ecosystem services and valuation of urban forests in China. Cities. 2009; 26: 187–194.
[20] Li YY, Shao MA. Change of soil physical properties under long-term natural vegetation restoration in the Loess Plateau of China. Journal of Arid Environments. 2006; 64: 77–96.
[21] Liu G, Jiang N, Zhang L, Liu Z. Soil physical and chemical analysis and description of soil profiles. Beijing: China Standard Methods Press. 1996.
[22] Ogaya R, Peñuelas J. Tree growth, mortality, and above-ground biomass accumulation in a holm oak forest under a five-year experimental field drought. Plant Ecology. 2007; 189: 291–299.
[23] Jose S. Agroforestry for ecosystem services and environmental benefits: an overview. Agroforestry Systems. 2009; 76: 1–10.
[24] Cabral I, Keim J, Engelmann R, Kraemer R, Siebert J, Bonn A. Ecosystem services of allotment and community gardens: A Leipzig, Germany case study. Urban Forestry & Urban Greening. 2017; 23: 44–53.
[25] Gan Y. The traits of Elaeocarpus sylvestris plantation and its influence on soils. Fujian Forestry. 2016; 3: 24–39.
[26] Li B. Growth characteristics of Elaeocarpus sylvestris plantation and its impact on the soil in Guangdong, China. Technology of Protection Forest. 2019; 6: 26–28.
[27] King DA. Tree form, height growth, and susceptibility to wind damage in Acer saccharum. Ecology. 1986; 67: 980–990.
[28] Kakareko G, Jung S, Ozguven EE. Estimation of tree failure consequences due to high winds using convolutional neural networks. International Journal of Remote Sensing. 2020; 41: 9039–9063.
[29] Zhang C, Stratópoulos LMF, Xu C, Pretzsch H, Rötzer T. Development of fine root biomass of two contrasting urban tree cultivars in response to drought stress. Forests. 2020; 11: 108.
[30] Iversen CM, McCormack ML, Powell AS, Blackwood CB, Freschet GT, Kattge J, *et al.* A global Fine-Root Ecology Database to address below-ground challenges in plant ecology. New Phytologist. 2017; 215: 15–26.
[31] Sprunger CD, Oates LG, Jackson RD, Robertson GP. Plant community composition influences fine root production and biomass allocation in perennial bioenergy cropping systems of the upper Midwest, USA. Biomass and Bioenergy. 2017; 105: 248–258.
[32] Aragão L, Malhi Y, Metcalfe D, Silva-Espejo JE, Jiménez E, Navarrete D, *et al.* Above-and below-ground net primary productivity across ten Amazonian forests on contrasting soils. Biogeosciences. 2009; 6: 2759–2778.
[33] Bardgett RD, Wardle DA, Yeates GW. Linking above-ground and below-ground interactions: how plant responses to foliar herbivory influence soil organisms. Soil Biology and Biochemistry. 1998; 30: 1867–1878.
[34] Goudriaan J, Van Laar H, Van Keulen H, Louwerse W. Photosynthesis, CO2 and plant production. Wheat Growth and Modelling. 1985; 107–122.
[35] Boots B, Russell CW, Green DS. Effects of microplastics in soil ecosystems: above and below ground. Environmental Science & Technology. 2019; 53: 11496–11506.
[36] Freschet GT, Violle C, Bourget MY, Scherer-Lorenzen M, Fort F. Allocation, morphology, physiology, architecture: The multiple facets of plant above- and below-ground responses to resource stress. New Phytologist. 2018; 219: 1338–1352.
[37] Esnard A-M, Sapat A. Displaced by disaster: Recovery and resilience in a globalizing world. London: Routledge. 2014.
[38] Gewin V. Food: an underground revolution. Nature News. 2010; 466: 552–553.
[39] Pierret A, Maeght J-L, Clément C, Montoroi J-P, Hartmann C, Gonkhamdee S. Understanding deep roots and their functions in ecosystems: an advocacy for more unconventional research. Annals of Botany. 2016; 118: 621–635.
[40] Liang J, Li B, Weng S, Fan T. Study on Growth and Biomass of 3 Species of Landscape Tree Seedlings. Subtropical Plant Science. 2017; 46: 231–235. (In Chinese)
[41] Kamimura K, Kitagawa K, Saito S, Mizunaga H. Root anchorage of hinoki (Chamaecyparis obtuse (Sieb. Et Zucc.) Endl.) under the combined loading of wind and rapidly supplied water on soil: analyses based on tree-pulling experiments. European Journal of Forest Research. 2012; 131: 219–227.
[42] Chang K-T, Chiang S-H, Hsu M-L. Modeling typhoon-and earthquake-induced landslides in a mountainous watershed using logistic regression. Geomorphology. 2007; 89: 335–347.
[43] Leuschner C, Hertel D, Schmid I, Koch O, Muhs A, Hölscher D. Stand fine root biomass and fine root morphology in old-growth beech forests as a function of precipitation and soil fertility. Plant and Soil. 2004; 258: 43–56.
[44] Ceccanti B, Masciandaro G, Garcia C, Macci C, Doni S. Soil bioremediation: combination of earthworms and compost for the ecological remediation of a hydrocarbon polluted soil. Water, air, and soil pollution. 2006; 177: 383–397.
[45] Zhou Q, Wei S, Diao C. Basic principles and researching progresses in ecological remediation of contaminated soils. Agro-Environmental Science. 2007; 26: 419–424.
[46] Tripathi V, Dubey RK, Edrisi SA, Narain K, Singh H, Singh N, *et al.* Towards the ecological profiling of a pesticide contaminated soil site for remediation and management. Ecological Engineering. 2014; 71: 318–325.
[47] Jia YB, Yang XE, Feng Y, Jilani G. Differential response of root morphology to potassium deficient stress among rice genotypes varying in potassium efficiency. Journal of Zhejiang University Science. 2008; 9: 427–434.
[48] Li Z, Fang W, Lu D. Physical and chemical properties of soils in Heshan hilly land. Acta Ecologica Sinica. 1995; 15: 93–102.
[49] Perera A, Nik VM, Chen D, Scartezzini J-L, Hong T. Quantifying the impacts of climate change and extreme climate events on energy systems. Nature Energy. 2020; 5: 150–159.
[50] Meir T, Orton PM, Pullen J, Holt T, Thompson WT, Arend MF. Forecasting the New York City urban heat island and sea breeze during extreme heat events. Weather and Forecasting. 2013; 28: 1460–1477.
[51] Lin L, Gao T, Luo M, Ge E, Yang Y, Liu Z, *et al.* Contribution of urbanization to the changes in extreme climate events in urban agglomerations across China. Science of the Total Environment. 2020; 744: 140264.
[52] Kocatepe A, Ulak MB, Kakareko G, Ozguven EE, Jung S, Arghandeh R. Measuring the accessibility of critical facilities in the presence of hurricane-related roadway closures and an approach for predicting future roadway disruptions. Natural Hazards. 2019; 95: 615–635.
[53] Zhang C, Stratopoulos LMF, Pretzsch H, Rötzer T. How do Tilia cordata Greenspire trees cope with drought stress regarding their biomass allocation and ecosystem services? Forests. 2019; 10: 676.

Keywords: Ecological remediation; Root development; Soil properties; Tree growth; Urban trees

Send correspondence to: Qing Zhao, Guangdong Academy of Forestry, Guangdong Provincial Key Laboratory of Silviculture Protection and Utilization, 510520 Guangzhou, Guangdong, China, E-mail: zhaoqing@sinogaf.cn